

Towards anisotropic spinfoam cosmology

Julian Rennert^{1,2*} and David Sloan^{3†}

¹ *Centre de Physique Théorique 1, CNRS-Luminy, Case 907, F-13288 Marseille*

² *Institut für Theoretische Physik, Universität Heidelberg,
Philosophenweg 16, D-69120 Heidelberg*

³ *DAMTP, Center for Mathematical Sciences,
Cambridge University, Cambridge CB3 0WA, UK*

We examine spinfoam cosmology by use of a simple graph adapted to homogeneous cosmological models. We calculate dynamics in the isotropic limit, and provide the framework for the anisotropic case. The dynamical behaviour is calculating transition amplitudes between holomorphic coherent states on a single node graph. The resultant dynamics is peaked on solutions which have no support on the zero volume state, indicating that big bang type singularities are avoided within such models.

PACS numbers: 04.60.Pp, 04.60.Kz, 98.80.Qc

arXiv:1304.6688v1 [gr-qc] 24 Apr 2013

*Electronic address: Rennert@stud.uni-heidelberg.de

†Electronic address: djs228@hermes.cam.ac.uk

I. INTRODUCTION

Cosmological models within the spinfoam framework serve a dual purpose [1]: Their primary function is to form a proposal for extracting cosmological predictions from a full theory of quantum gravity. These models also perform a useful secondary role in forming a bridge between the canonical [2] and covariant [3] formulations of Loop Quantum Gravity (LQG). The covariant, or spinfoam, approach is a ‘bottom up’ construction - one predicates a quantum model and thence derives dynamics. As such the existence of a semi-classical limit and its agreement with the predictions of General Relativity are not a foregone conclusion, but rather must be examined within physical scenarios. This situation contrasts that of Loop Quantum Cosmology (LQC) [4], the application of the principles of LQG to cosmological mini-superspaces.

Another important question that has to be clarified by spinfoam cosmology is whether physical predictions such as the resolution of cosmological singularities, a well trusted result in LQC [5] [6], can also be derived within this approach. The resolution of the big bang singularity, and its replacement with a deterministic bounce, is a key success of the canonical theory. It forms the basis of investigation of observable consequences of the theory [7] [8]. It is therefore a crucial test of the spinfoam approach that it reproduces these features in the ultraviolet sector.

In [1] it was shown how to calculate the transition amplitude between two quantum states of gravity in the homogeneous and isotropic cosmological regime using a simple two-node graph (the dipole graph) at the first order in the vertex expansion. The main result of this work was to demonstrate that the used new spinfoam vertex amplitude (EPRL/KKL), [9–12], together with some other ingredients, are adequate to derive a classical limit which can be identified with the Friedmann dynamics of an empty flat, homogeneous and isotropic universe, i.e. Minkowski space. This result was further strengthened in [13], where a slight modification of the spinfoam vertex was utilized to implement a cosmological constant and derive a de Sitter universe as the classical limit. However, despite these original results being interesting, they exhibit a considerable deficiency, namely they fail to reproduce the curvature term $\frac{k}{a^2}$, which appears in the Friedmann equation. Such a term is expected, since the chosen graph is dual to a (degenerate) triangulation of the three sphere, (the closed topology, in which $k = 1$). The authors of [1] argue that this term might be recovered by taking higher orders of the spin approximation into account. However, this term appears in a more natural manner, as we will show in section II C.

Our approach is the following: We will examine flat ($k = 0$) Friedmann-Lemâitre-Robertson-Walker (FLRW) models by use of a simple graph. This ‘Daisy’ graph consists of a single node which is both the source and target of three links. This graph can be thought of in two equivalent ways: In the first instance one has tessellated space by identical cubes, and so by symmetry opposite faces of a cube are identified, thus an outgoing edge dual to a given face is an incoming edge dual to the opposite face. The second instance is to consider the spatial slice to be a flat three-torus, with each link transcribing a compact direction. This is what separates this approach from the cubulation used in [14] and also in [15].

The second motivation is to provide the framework for investigating the more complicated case of Bianchi cosmologies. Since the inclusion of matter within the spinfoam paradigm has not yet been realized, one can only investigate FLRW models with trivial classical dynamics. In the anisotropic homogeneous systems comprising the Bianchi models there is a rich physical evolution even in the absence of any matter. These models have been

examined extensively in LQC, both within the quantum framework [16], [17], [18] and the semi-classical effective framework [19], [20], [21].

II. RECAP OF THE THEORETICAL FRAMEWORK

Let us briefly review the necessary theoretical input to make our ideas and calculations tractable, and fix our notation. Since we rely heavily on the theory as introduced in [1] we refer the reader to the original source or [3, 22] for a more detailed discussion.

A. LQG and spinfoams

The kinematical Hilbert space of LQG is defined as the direct sum of subspaces \mathcal{H}_Γ over all graphs Γ , embedded in a three dimensional manifold Σ . Since we want to work in a cosmological regime, describing just a finite number of degrees of freedom, it is sufficient for us to consider just one of these subspaces. This Hilbert space \mathcal{H}_Γ is defined on a graph Γ with L links and N nodes. Its elements are the spin network functions; gauge invariant, square integrable functions $\Psi : SU(2)^L \rightarrow \mathbb{C}$, (*holonomy representation*). Since gauge transformations act on the nodes N the Hilbert space \mathcal{H}_Γ is given by

$$\mathcal{H}_\Gamma = \mathcal{L}^2(SU(2)^L / SU(2)^N). \quad (2.1)$$

The name holonomy representation results from the circumstance that the $SU(2)$ elements h_l are the holonomy of the Ashtekar-Barbero connection along the link l , i.e.

$$h_l = h_l(A) = \mathcal{P} \exp \left(\int_l A \right) \quad (2.2)$$

with $A = A_a^i \tau^i dx^a$. The components of A are given by $A_a^i = \Gamma_a^i + \gamma K_a^i$ with Γ_a^i being the spin-connection, K_a^i the extrinsic curvature of Σ and $\gamma \in \mathbb{R}_{>0}$ is the Barbero-Immirzi parameter. Thus the $SU(2)$ elements h_l contain the geometrical information of the quantum state $\Psi(h_l)$.

Another representation, related to the former one via the Peter-Weyl transformation [3, 23], is the spin-intertwiner representation. In this representation the graph Γ carries spins $j_l \in \frac{\mathbb{N}}{2}$ at each link and invariant tensors i_n , called intertwiners, at each node. Those spins correspond to the spins of the unitary irreducible representations of $SU(2)$ and the intertwiners belong to the $SU(2)$ -invariant subspace $\mathcal{K}_n = \text{Inv}_{SU(2)}[\mathcal{H}_n]$, where \mathcal{H}_n is the tensor product of the representation spaces carried by the links meeting at the node n , $\mathcal{H}_n = \otimes_{l \in n} \mathcal{H}_{j_l}$. A general state in \mathcal{H}_Γ has the following structure in the spin-intertwiner representation

$$\Psi_{j_l, i_n}(h_l) = \left(\bigotimes_n i_n \right) \cdot \left(\bigotimes_l \mathcal{D}^{(j_l)}(h_l) \right), \quad (2.3)$$

where $\mathcal{D}^{(j_l)}(h_l)$ is the $2j_l + 1$ dimensional Wigner matrix of the holonomy h_l and the dot indicates contraction of indices.

There are two interpretations of the role of the 3-dim. manifold Σ in which Γ lives: The original is that Σ is a spacelike slice at some coordinate time t . The spinfoam model would then define a transition amplitude from $\mathcal{H}_{\Gamma(\Sigma_t)}$ to $\mathcal{H}_{\Gamma(\Sigma_{t+1})}$. This picture, making use of

this time t , however, is not well suited if we want to preserve full 4-dim. diffeomorphism invariance. Thus, the second interpretation holds Σ to be a 3-dim. boundary of a 4-dim. spacetime region. The states in $\mathcal{H}_{\Gamma(\Sigma)}$ are thus not thought of as ‘states at some time’, but rather as *boundary states*, [3].

The dynamics of these quantum states can be defined via the spinfoam formalism. Think again of a boundary state $\Psi \in \mathcal{H}_{\Gamma}$ with $\Gamma \subset \Sigma$. A spinfoam lives on a 2-complex made up of vertices, edges and faces. A 2-complex can be seen as a discretization of 4-dim. spacetime and heuristically may be thought of as resulting from a spin network evolving in time. A spinfoam model now assigns an amplitude to the state Ψ in the following way

$$\langle W | \Psi \rangle = \sum_{\sigma} \prod_v W_v(\sigma) \quad (2.4)$$

where the sum is over different spin network histories and $W_v(\sigma)$ is called the vertex amplitude. We will present its precise structure in section III where we again will follow closely [1].

B. Coherent states

Coherent states are an important tool for the examination of the classical limit of any quantum theory. In this section we will summarize a few definitions about the coherent states for LQG. In particular we will use the Livine-Speziale coherent intertwiners [24] as well as the coherent states in the holomorphic representation [23, 25] later in this work.

The Livine-Speziale coherent intertwiners make use of the Perelomov coherent states for $SU(2)$ such that the intertwiner i_n in (2.3) is replaced by a coherent intertwiner. A Perelomov coherent state for $SU(2)$ takes the highest weight state $|j, j\rangle \in \mathcal{H}^{(j)}$, which is a coherent state along \hat{e}_z , and rotates it with a Wigner matrix $\mathcal{D}^{(j)}(h_{\vec{n}})$ such that it is coherent along another axis \vec{n} . The element $h_{\vec{n}} \in SU(2)$ corresponds to the $SO(3)$ element $R_{\vec{n}}$ that rotates \hat{e}_z into \vec{n} . Thus we obtain the coherent state $|j, \vec{n}\rangle \equiv \mathcal{D}^{(j)}(h_{\vec{n}})|j, j\rangle$. Consider a node n which joins E links e together. A coherent intertwiner at this node n is now given by the tensor product of the coherent states coming from each single link. The gauge invariance of these states is achieved via group integration.

$$\Phi_n(\vec{n}_e) = \int_{SU(2)} dg \bigotimes_{e=1}^E \mathcal{D}^{(j_e)}(g) |j_e, \vec{n}_e\rangle \quad (2.5)$$

The holomorphic coherent states are characterized by an element $H_l \in SL(2, \mathbb{C})$ given at each link of the graph Γ . They are defined by

$$\Psi_{H_l}(h_l) = \int_{SU(2)^N} dg_n \prod_l K_t(g_{s(l)} h_l g_{t(l)}^{-1}, H_l), \quad (2.6)$$

where K_t is the analytic continuation of the $SU(2)$ heat kernel to $SL(2, \mathbb{C})$ and the group integration again ensures gauge invariance. The heat kernel is given by

$$K_t(a, B) = \sum_{j \in \mathbb{N}_0/2} (2j+1) e^{-\alpha t j(j+1)} \text{Tr}(\mathcal{D}^{(j)}(aB^{-1})) \quad (2.7)$$

with $a \in SU(2)$, $B \in SL(2, \mathbb{C})$ and $\alpha, t \in \mathbb{R}_{>0}$. The $SL(2, \mathbb{C})$ label H_l now allows for two different decompositions [23]. The first one is the polar decomposition

$$H_l = h_l(A) \exp \left(i \frac{E_l}{8\pi G \hbar \gamma} t_l \right) \quad (2.8)$$

and shows clearly that H_l determines a point in classical phase space on which the coherent state is peaked. $h_l \in SU(2)$ is the holonomy of the Ashtekar connection A_a^i and $E_l \in \mathfrak{su}(2)$ is the flux of the densitized triad E_i^a . Thus, a coherent state with label (2.8) corresponds to a classical configuration (A_a^i, E_i^a) .

The second decomposition of H_l uses two $SU(2)$ elements $h_{\vec{n}_l}$ and $h_{\vec{n}'_l}$ which, analogously to the $SU(2)$ elements of the Perelomov coherent states, correspond to the transformation of \hat{e}_z into \vec{n}_l and \vec{n}'_l . Furthermore, a complex number z_l is used whose real part is associated to the extrinsic curvature and its imaginary part is related to the area that is pierced by the link l [23].

$$H_l = h_{\vec{n}_l} e^{-iz_l \frac{\sigma^3}{2}} h_{\vec{n}'_l}^{-1} \quad (2.9)$$

We denote the real and the imaginary part of z_l as $z_l = c_l + ip_l$ and σ^3 is the third Pauli matrix. The relation between the two decompositions becomes clear by writing (2.9) in the polar decomposition. One finds that [23]

$$h_l = h_{\vec{n}_l} e^{-ic_l \frac{\sigma^3}{2}} h_{\vec{n}'_l}^{-1}, \quad (2.10)$$

$$E_l = \int_{f_l} E = 8\pi G \hbar \gamma p_l \vec{n}'_l \cdot \frac{i\vec{\sigma}}{2t_l}. \quad (2.11)$$

Where f_l is the face dual to the link l with area $\mathcal{A}_l = 8\pi G \hbar \gamma p_l / t_l$.

C. Classical preliminaries

We are interested in the applicability of spinfoam cosmology to homogeneous models, both in the isotropic and anisotropic cases. In this section we will establish the holonomies and the fluxes for such models. We assume our spacetime to be of the form $\mathcal{M} = \mathbb{R} \times \Sigma$, with Σ being a homogeneous 3-space. Under the additional assumption of isotropy the metric of \mathcal{M} can be given by

$$ds^2 = -dt^2 + a(t)^2 d\Omega^2 \quad (2.12)$$

with $d\Omega^2 = dr^2/(1 - kr^2) + r^2 d\theta^2 + r^2 \sin^2 \theta d\phi^2$ and $k \in \{0, \pm 1\}$. The parameter k distinguishes three different spaces with constant curvature, where we are interested in the closed ($k = 1$) and the flat ($k = 0$) case. The flat and closed universes are special cases of the Bianchi I and IX universes respectively, in which all scale factors have been identified. If we consider a universe without matter but just a cosmological constant Λ , the metric (2.12) evolution obeys the Friedmann equation

$$\left(\frac{\dot{a}}{a} \right)^2 + \frac{k}{a^2} = \frac{\Lambda}{3}. \quad (2.13)$$

In the case of vanishing cosmological constant the only possible solution is a static spacetime $a(t) = \text{const.}$, where for $k = 0$ one recovers Minkowski space. If $\Lambda \neq 0$ one obtains

for $k = 0$, and under the assumption that $a(t) \gg 1$ also for $k = 1$, the *de Sitter solution*, $a(t) = \exp(\pm\sqrt{\Lambda/3}t)$.

If we drop the restriction to isotropic models we obtain a Bianchi I universe in the flat case, which is described by the following line element

$$ds^2 = -dt^2 + a_1(t)^2 dx^2 + a_2(t)^2 dy^2 + a_3(t)^2 dz^2. \quad (2.14)$$

Considering again a vacuum spacetime (with $\Lambda = 0$), the three directional scale factors a_1, a_2, a_3 have to satisfy

$$a_1 \dot{a}_2 \dot{a}_3 + a_2 \dot{a}_1 \dot{a}_3 + a_3 \dot{a}_1 \dot{a}_2 = 0. \quad (2.15)$$

This equation is solved by the so called *Kasner universe* and is given by $a_i(t) \propto t^{\kappa_i}$. The Kasner exponents have to fulfill the conditions $\sum_i \kappa_i^2 = \sum_i \kappa_i = 1$. From those conditions one deduces that one exponent has to be negative, while the other two are positive which leads to a contraction in one direction and an expansion in the other two.

Now, in order to specify the holonomy and the flux, we need the Ashtekar connection and the corresponding densitized triad. For that we will use the results provided in [5, 26–28].

In a general, i.e. non-cosmological, setting the Ashtekar connection is given by $A_a^i = \Gamma_a^i + \gamma K_a^i$, with K_a^i being related to the extrinsic curvature

$$K_a^i = e^{ib} K_{ab} = \frac{1}{2} e^{ib} \mathcal{L}_{(\frac{\partial}{\partial t})} h_{ab}, \quad (2.16)$$

where the e_a^i are co-triads, such that the spatial metric can be expressed as $h_{ab} = \delta_{ij} e_a^i e_b^j$. The connection coefficients Γ_a^i are calculated via contraction of the spin connection $\Gamma_a^i = -\frac{1}{2} \varepsilon^{ijk} \theta_{ajk}$, which is given by

$$\theta_{aj}^i = -e_j^b (\partial_a e_b^i - \Gamma_{ab}^c e_c^i). \quad (2.17)$$

Γ_{ab}^c is the Levi-Civita connection compatible with h_{ab} , expressed in terms of the co-triads. However, using the framework of invariant connections on principal fibre bundles, as explained in [26], simplifies the tedious calculation of A_a^i via (2.16) and (2.17) enormously. Now, a Bianchi model is a symmetry reduced model of general relativity by a symmetry group S , which acts freely and transitively on Σ . If Σ is invariant under the action of S it is an homogeneous 3-space and a connection can be decomposed as $A_a^i = \phi_I^i \omega_a^I$, with left invariant 1-forms ω_a^I and constant coefficients ϕ_I^i . A further reduction, which leaves us for example with the three gauge invariant degrees of freedom in (2.15), is achieved by diagonalizing ϕ_I^i . This has the effect that we can write

$$A_a^i = c_{(K)} \Lambda_K^i \tilde{\omega}_a^K, \quad (2.18)$$

with $\Lambda_K^i \in SO(3)$, [5]. Using the left-invariant vector fields X_I^a , dual to the 1-forms ω_a^I , allows us to decompose also the densitized triad as

$$E_i^a = p_i^I X_I^a = p^{(K)} \Lambda_K^i \tilde{X}_K^a, \quad (2.19)$$

where the second equality results again from a diagonalization of p_i^I . These six coefficients (c_K, p^K) , $K = 1, 2, 3$ now span the phase space of our reduced homogeneous model with the symplectic structure [16]

$$\{c_I, p^J\} = \frac{8\pi G}{3} \gamma \delta_I^J. \quad (2.20)$$

If we expand the co-triads as $e_a^i = e_{(K)} \Lambda_K^i \tilde{\omega}_a^K$, with arbitrary $e_K \in \mathbb{R}$, we get the following relations (no summation)

$$p^I = |\varepsilon_{IJK} e_J e_K| \operatorname{sgn}(e_I). \quad (2.21)$$

With these simplifications the connection components $\Gamma_a^i = \Gamma_{(I)} \Lambda_I^i \tilde{\omega}_a^I$ are given by, (no summation, even permutation of $\{1,2,3\}$)

$$\Gamma_I = \frac{1}{2} \left(\frac{p^K}{p^J} n^J + \frac{p^J}{p^K} n^K - \frac{p^J p^K}{(p^I)^2} n^I \right). \quad (2.22)$$

The n^I characterize our Bianchi model, we have for example $n^I = 0$ for Bianchi I and $n^I = 1$ for Bianchi IX. Thus, we see that the Bianchi I models have vanishing spin connection Γ_a^i . The extrinsic curvature is given by $K_I = \frac{1}{2} \dot{e}_I$, [5], where the dot indicates a derivative with respect to the coordinate time t . Now, we find the following results for the Ashtekar connection in the homogeneous setting

$$A_a^i = c_{(I)} \Lambda_I^i \tilde{\omega}_a^I = \left(\Gamma_{(I)} + \frac{\gamma}{2} \dot{e}_{(I)} \right) \Lambda_I^i \tilde{\omega}_a^I. \quad (2.23)$$

In the isotropic case we have $p^1 = p^2 = p^3$ and (2.22) gives us $\Gamma_I = 0$ in the flat case (Bianchi I), whereas we get $\Gamma_I = \frac{1}{2}$ in the model with positive curvature (Bianchi IX). We can thus write $c = \frac{1}{2}(k + \gamma \dot{e})$, $k \in \{0, 1\}$. For the anisotropic (Bianchi I) model we get $c_I = \frac{\gamma}{2} \dot{e}_I$.

Before we apply this formalism to our one-node graph let us make the following observation. In [1] it was shown that the holomorphic transition amplitude between two homogeneous and isotropic quantum states, which are supposed to correspond to a curved geometry ($k = 1$), is given by

$$W(z) = N z \exp \left(-\frac{z^2}{2t\hbar} \right). \quad (2.24)$$

Following the reasoning in [13] the main contribution of $W(z)$ is obtained when the real part of z^2 vanishes and its imaginary part is proportional to πl , $l \in \mathbb{Z}$. Now, if we use the correct relation between c and the metric variables, i.e. $c = \operatorname{Re}(z) = \frac{1}{2}(k + \gamma \dot{a})$, instead of just $c = \dot{a}$ we can reproduce the correct Hamiltonian constraint. Therefore, we require that the real and the imaginary part (which doesn't contribute anyway, if we consider $|W(z)|$) vanish. Thus, we get from $z^2 = (c + ip)^2$

$$c^2 - p^2 \stackrel{!}{=} 0. \quad (2.25)$$

However, the p^2 term will disappear if we consider the proper normalized amplitude as done in [13] or [29]. Thus, we find $c^2 = 0$ and

$$\begin{aligned} c^2 &= \frac{1}{2} \left(\frac{1}{2} + \gamma \dot{a} + \frac{\gamma^2 \dot{a}^2}{2} \right) = 0 \\ &= \frac{1}{2} (1 + \gamma \dot{a}) - \frac{1}{4} (1 - \gamma^2 \dot{a}^2) \\ &= c - \frac{1}{4} (1 - \gamma^2 \dot{a}^2) \end{aligned} \quad (2.26)$$

$$\Rightarrow -\frac{1}{4} (1 - \gamma^2 \dot{a}^2) = 0 \quad (2.27)$$

Scaling of \dot{a} and multiplication by a gives us

$$-\dot{a}^2 a + a = 0 \quad (2.28)$$

which is, up to constants, the right Hamiltonian constraint for a curved FLRW universe.

We have already mentioned the definition of the holonomy in (2.2). Now, let us define the flux. If we denote the link along which we evaluate the holonomy by l then S_l denotes a surface pierced by l . One says S is dual to l . The flux of the electric field $E = E_i \tau^i X_a$ through a surface S_l is given by

$$E(S) = \int_{S_l} (*E)^j n^j, \quad (2.29)$$

where $*$ denotes the Hodge dual, which converts our vector E into a 2-form, ($\dim(\Sigma) = 3$), and $n^j = n^i \tau^i$ is a $\mathfrak{su}(2)$ valued scalar smearing function [30]. We will use the definition

$$(*E) = (*E)^j \tau^j = (*E)_{a_1 a_2}^j dx^{a_1} \wedge dx^{a_2} \tau^j \quad (2.30)$$

with

$$(*E)_{a_1 a_2}^j = \varepsilon_{aa_1 a_2} E_j^a. \quad (2.31)$$

These definitions will become necessary especially for the anisotropic case, when we explicitly have to calculate the Ashtekar connection and the flux for our model.

III. OUR MODEL

We want to calculate in this section the transition amplitude between two flat, homogeneous and isotropic universes. Therefore, we think of a cubical partition of 3-space Σ . The dual graph (with toroidal topology) is then given by the *Daisy graph*, see FIG.(1). We will work in the one-vertex spinfoam expansion and we will use the coherent states in the holomorphic representation. The original motivation for this graph was its potential applicability to anisotropic cosmological settings and therewith a physically more interesting situation, a problem we will tackle in a followup paper. In this first paper we will restrict our attention mostly to the isotropic case and see that this one vertex graph is sufficient to reproduce the original result of [1].

A. The Setting

First, let us recall the definition for the vertex amplitude to specify the dynamics. Despite it being shown in [31] that there exist additional 2-complexes with the same boundary graph already at the one vertex level (for the dipole graph) we will consider just one spinfoam in the sum in (2.4). We consider the spinfoam that simply connects the two graph vertices with a single spinfoam vertex. The one vertex spinfoam expansion ($v = 1$) leads to the factorization of our amplitude $W_v(\sigma)$, [1, 32]. With these simplifications and following [1] the transition amplitude between an initial and a final geometry is given by

$$W(\Psi_f, \Psi_i) = W_f(H_l(z_f)) W_i(H_l(z_i)), \quad (3.1)$$

where the single factors are

$$W(z) = \int_{G^N} dG_n \prod_l K_t(H_l(z), G_{s(l)} G_{t(l)}^{-1}) \quad (3.2)$$

where $K_t(H_l(z), G)$ is defined in (2.7) and G is $SO(4)$ for the Euclidean theory and $SL(2, \mathbb{C})$ for the Lorentzian theory, respectively. As was explained in [33] for the Lorentzian case we will neglect one integration so that $W(z)$ does not diverge. Furthermore, since our graph has just one node we find that source and target node of each link are the same, i.e. $s(l) = t(l)$, thus leading to $G_{s(l)} G_{t(l)}^{-1} = \mathbb{I}$.

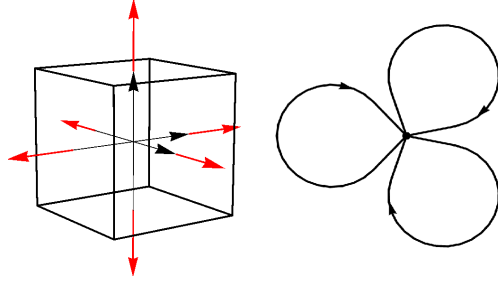


FIG. 1: Cube and Daisy graph

A clear advantage of using this graph is its simple application in the homogeneous case. It allows us to explicitly calculate the $SL(2, \mathbb{C})$ elements for our coherent states and with that provides helpful insights also for more complicated structures. We begin by calculating the $SL(2, \mathbb{C})$ elements $H_l(z)$ using the decomposition (2.9)

$$H_l(z) = u_l e^{-iz \frac{\sigma^3}{2}} \tilde{u}_l^{-1}, \quad (3.3)$$

where u_l and \tilde{u}_l are elements of $SU(2)$. We have three links, l_1, l_2, l_3 and six normal vectors $n_1 = \hat{e}_x$ and $\tilde{n}_1 = -\hat{e}_x$, $n_2 = \hat{e}_y$ and $\tilde{n}_2 = -\hat{e}_y$ and $n_3 = \hat{e}_z$ and $\tilde{n}_3 = -\hat{e}_z$. The normal vectors n_l and \tilde{n}_l are obtained via a $SO(3)$ transformation of \hat{e}_z and the $SU(2)$ elements u_l and \tilde{u}_l are related to these $SO(3)$ transformations, cf. appendix A. Now, we have to bring the three $SL(2, \mathbb{C})$ elements in the following form

$$H_l(z) = e^{-i\alpha_1 \frac{\sigma^3}{2}} e^{-i\beta \frac{\sigma^2}{2}} e^{-i\alpha_2 \frac{\sigma^3}{2}}. \quad (3.4)$$

This means that we have to find the angles α_1, α_2 and β . Given the $SL(2, \mathbb{C})$ elements $H_l(z)$ in this form we are then able to represent their Wigner matrices for all j if we recall that the angular momentum operators $\hat{J}_x, \hat{J}_y, \hat{J}_z$ are given by $\hat{J}_x = \frac{\sigma^1}{2}$, $\hat{J}_y = \frac{\sigma^2}{2}$ and $\hat{J}_z = \frac{\sigma^3}{2}$ in the $j = \frac{1}{2}$ representation. Hence, we get

$$\mathcal{D}^{(j)}(H_l(z)) = e^{-i\alpha_1 \hat{J}_z^{(j)}} e^{-i\beta \hat{J}_y^{(j)}} e^{-i\alpha_2 \hat{J}_z^{(j)}}. \quad (3.5)$$

One finds the following angles (cf. equation (A14), (A15), (A16) in the appendix)

$$H_1(z) : \quad \alpha_1 = \alpha_2 = \frac{\pi}{2} \quad , \quad \beta = \pi - z \quad (3.6)$$

$$H_2(z) : \quad \alpha_1 = \pi \quad , \quad \alpha_2 = 0 \quad , \quad \beta = \pi - z \quad (3.7)$$

$$H_3(z) : \quad \alpha_1 = z \quad , \quad \alpha_2 = 0 \quad , \quad \beta = 0 \quad (3.8)$$

We can now calculate the transition amplitude $W(z) =$

$$\int_G dG \prod_{l=1}^3 \sum_j d_j e^{-2thj(j+1)} \text{Tr} \left(\mathcal{D}^{(j)}(H_l(z)) \tilde{G} \right), \quad (3.9)$$

where we have defined $d_j = 2j+1$ and $\tilde{G} \equiv Y^\dagger \mathcal{D}^{(j^+, j^-)}(G_s G_t^{-1}) Y$ in the case of Euclidean gravity, ($G \in SO(4)$), or $\tilde{G} \equiv Y^\dagger \mathcal{D}^{(\gamma j, j)}(G_s G_t^{-1}) Y$ in the Lorentzian case, ($G \in SL(2, \mathbb{C})$). For detail cf. [3]. (Despite $GG^{-1} = \mathbb{I}$, because $s(l) = t(l)$ as mentioned earlier, we keep \tilde{G} for completeness.) Lets start by calculating the trace for $l = 1$

$$\begin{aligned} \text{Tr} \left(\mathcal{D}^{(j)}(H_1(z)) \tilde{G} \right) &= \sum_{m=-j}^j \langle j, m | \mathcal{D}^{(j)}(H_1(z)) \tilde{G} | j, m \rangle \\ &= \sum_{m, k=-j}^j e^{-i(m+k)\frac{\pi}{2}} d_{mk}^{(j)}(\pi - z) \langle j, k | \tilde{G} | j, m \rangle, \end{aligned} \quad (3.10)$$

where we have inserted a unit operator. This leads to a separation of the geometrical information, stored in $H_l(z)$, and the gauge invariant contribution, given by $\langle j, k | \tilde{G} | j, m \rangle$. For simplicity we will neglect the gauge contribution later on. For a detailed way of dealing with the trace cf. [29].

For $l = 2$ we get analogously

$$\begin{aligned} \text{Tr} \left(\mathcal{D}^{(j)}(H_2(z)) \tilde{G} \right) &= \sum_{m=-j}^j \langle j, m | \mathcal{D}^{(j)}(H_2(z)) \tilde{G} | j, m \rangle \\ &= \sum_{m, k=-j}^j e^{-i\pi m} d_{mk}^{(j)}(\pi - z) \langle j, k | \tilde{G} | j, m \rangle \end{aligned} \quad (3.11)$$

and for $l = 3$

$$\begin{aligned} \text{Tr} \left(\mathcal{D}^{(j)}(H_3(z)) \tilde{G} \right) &= \sum_{m=-j}^j \langle j, m | \mathcal{D}^{(j)}(H_3(z)) \tilde{G} | j, m \rangle \\ &= \sum_{m, k=-j}^j e^{-izm} \langle j, k | \tilde{G} | j, m \rangle. \end{aligned} \quad (3.12)$$

We will now use the large volume approximation, i.e. for $\text{Im}(z) \gg 1$ the term with $m = j$ dominates.

$$\text{Tr} \left(\mathcal{D}^{(j)}(H_3(z)) \tilde{G} \right) \approx \sum_{k=-j}^j e^{-izj} \langle j, k | \tilde{G} | j, j \rangle. \quad (3.13)$$

Now, how do we treat the links $l = 1$ and $l = 2$? One can argue, that due to the highly symmetric setting we should also use $m = j$ for those cases. If we do so we can make use of the following asymptotic relation [34]

$$\begin{aligned} d_{jm}^{(j)}(\beta) &= (-1)^{j-m} \sqrt{\frac{(2j)!}{(j+m)!(j-m)!}} \times \\ &\times [\cos(\beta/2)]^{j+m} [\sin(\beta/2)]^{j-m}. \end{aligned} \quad (3.14)$$

So lets start with $l = 1$. For $m = j$ we get

$$\begin{aligned} \text{Tr} \left(\mathcal{D}^{(j)}(H_1(z)) \tilde{G} \right) &\approx \\ \sum_{k=-j}^j e^{-i(j+k)\frac{\pi}{2}} d_{jk}^{(j)}(\pi - z) \langle j, k | \tilde{G} | j, j \rangle. \end{aligned} \quad (3.15)$$

By making use of

$$d_{mk}^{(j)}(\pi - z) = (-1)^{m-j} d_{m(-k)}^{(j)}(z) \quad (3.16)$$

and (3.14) we can analyse $d_{jk}^{(j)}(\pi - z)$ and get

$$\begin{aligned} d_{jk}^{(j)}(\pi - z) &= (-1)^{j-j} d_{j(-k)}^{(j)}(z) = d_{j(-k)}^{(j)}(z) \\ &= (-1)^{j+k} \sqrt{\frac{(2j)!}{(j-k)!(j+k)!}} \times \\ &\quad \times [\cos(z/2)]^{j-k} [\sin(z/2)]^{j+k} \end{aligned} \quad (3.17)$$

For the trigonometric functions we get for $\text{Im}(z) \gg 2$

$$\cos(z/2) \approx \frac{1}{2} e^{-iz/2}, \quad \sin(z/2) \approx \frac{i}{2} e^{-iz/2}, \quad (3.18)$$

which gives us the following expression

$$\begin{aligned} &[\cos(z/2)]^{j-k} [\sin(z/2)]^{j+k} \approx \\ &\left(\frac{1}{2}\right)^{j-k} \left(\frac{1}{2}\right)^{j+k} (i)^{j+k} e^{-i\frac{z}{2}(j-k)} e^{-i\frac{z}{2}(j+k)} \\ &= \left(\frac{1}{2}\right)^{2j} (i)^{j+k} e^{-izj}. \end{aligned} \quad (3.19)$$

We can use this to obtain

$$\begin{aligned} \text{Tr} \left(\mathcal{D}^{(j)}(H_1(z)) \tilde{G} \right) &\approx \left(\frac{1}{2}\right)^{2j} e^{-i(z+\frac{\pi}{2})j} \times \\ \sum_{k=-j}^j e^{-ik\frac{\pi}{2}} (-1)^{j+k} i^{j+k} &\sqrt{\frac{(2j)!}{(j-k)!(j+k)!}} \langle j, k | \tilde{G} | j, j \rangle. \end{aligned} \quad (3.20)$$

If we take the $e^{-i\frac{\pi}{2}j}$ term inside the sum we get $e^{-i\frac{\pi}{2}(k+j)} (-1)^{j+k} i^{j+k}$, which is equal to $(-1)^{2j+2k} i^{2j+2k}$, so we get

$$\begin{aligned} \text{Tr} \left(\mathcal{D}^{(j)}(H_1(z)) \tilde{G} \right) &\approx \left(\frac{1}{2}\right)^{2j} e^{-izj} \times \\ \sum_{k=-j}^j (-1)^{2j+2k} i^{2j+2k} &\sqrt{\frac{(2j)!}{(j-k)!(j+k)!}} \langle j, k | \tilde{G} | j, j \rangle. \end{aligned} \quad (3.21)$$

Now let us make a few comments about the last expression. First, notice that we can reproduce the factor e^{-izj} , which appears also in the original work [1] and is crucial for the derivation of the transition amplitude. The second point is that we can proceed by approximating also the second part, namely the sum over k , as $k = j$, which simplifies the result and the important thing is, that by doing this approximation we are not doing worse than the projection onto $m = j$ in the original work.

The calculation for $l = 2$ is identical to the case $l = 1$. If we now use the following two relations

$$\left(\frac{1}{2}\right)^{2j} = e^{\ln(1/4)j} \quad , \quad (-1)^{j+k} i^{j+k} = (-i)^{j+k} . \quad (3.22)$$

and apply the approximation $k = j$ we get (neglecting factors like $(-1)^{2j}$)

$$\begin{aligned} \text{Tr} \left(\mathcal{D}^{(j)}(H_1(z)) \tilde{G} \right) &\approx e^{-izj + \ln(\frac{1}{4})j} \langle j, j | \tilde{G} | j, j \rangle , \\ \text{Tr} \left(\mathcal{D}^{(j)}(H_2(z)) \tilde{G} \right) &\approx e^{-izj + \ln(\frac{1}{4})j} \langle j, j | \tilde{G} | j, j \rangle , \\ \text{Tr} \left(\mathcal{D}^{(j)}(H_3(z)) \tilde{G} \right) &\approx e^{-izj} \langle j, j | \tilde{G} | j, j \rangle . \end{aligned} \quad (3.23)$$

Now, let us compare these results with the calculations of the original paper [1]. There the authors used a projection onto the highest spin state $m = j$ and got a factor $\exp(-izj)$ for all links. Our calculation gives the same result using a simpler graph. Furthermore, due to our explicit calculation we see in a more precise way where this factor comes from. Now, the term $\langle j, j | \tilde{G} | j, j \rangle$ can be neglected in our case because $s(l) = t(l)$ and thus

$$\begin{aligned} \langle j, j | \tilde{G} | j, j \rangle &= \langle j, j | Y^\dagger \mathcal{D}^{(\gamma j, j)}(G_{s(l)} G_{t(l)}^{-1}) Y | j, j \rangle \\ &= \langle j, j | Y^\dagger \mathcal{D}^{(\gamma j, j)}(\mathbb{I}) Y | j, j \rangle \\ &= \langle (\gamma j, j), j, j | \mathbb{I} | (\gamma j, j), j, j \rangle = 1 , \end{aligned} \quad (3.24)$$

where we have used the projection property of the unitary Y -map, cf. [1]. In [1] the authors replaced the whole gauge contribution ($\langle j, j | \tilde{G} | j, j \rangle$) from all four links by a factor $\frac{N_0}{j^3}$ based on a calculation done in [24].

So far we have assumed that all our z -labels are the same for each link, which is a consequence of the isotropic configuration we are considering. If we investigate the anisotropic case these labels are going to be different $z = z_l$.

B. Results

Inserting the results for the traces given by (3.23) and (3.24) into the transition amplitude (3.9) we get

$$W(z) = \left(\sum_j (2j+1) e^{-2thj(j+1) - izj} \right)^3 . \quad (3.25)$$

Furthermore, we have assumed that $\text{Im}(z) = p \gg \ln(1/4) \approx -1.38$, which is justified since $p > 0$, and thus all three links give the same contribution.

Now we can either apply a gaussian approximation as was done in [1], we can investigate the amplitude numerically or we calculate (3.25) explicitly using the Cauchy product, all of which yield the same result. The gaussian approximation gives the result

$$W(z) = (2j_0 + 1)^3 \left(\sqrt{\frac{\pi}{2t\hbar}} \right)^3 e^{\frac{3(2t\hbar + iz)^2}{8t\hbar}}, \quad (3.26)$$

where j_0 is given by

$$j_0 = -\frac{1}{2} + \frac{\text{Im}(z)}{4t\hbar}. \quad (3.27)$$

In order to get meaningful results we now have to normalize the amplitude. For this we use the following expression for the norm of a heat kernel coherent state given on a single link [29]

$$\|\psi_g^{\tilde{t}}\| = \frac{4\sqrt{\pi}e^{\tilde{t}/4}}{\tilde{t}^{3/2}} \frac{1}{\sinh(\tilde{p})} \frac{\tilde{p}}{2} e^{\frac{\tilde{p}^2}{\tilde{t}}}, \quad (3.28)$$

where we have taken just the leading order term with $n = 0$, cf. [29]. The small g in the above formula corresponds to our $SL(2, \mathbb{C})$ element $H_l(z)$ and the heat kernel time \tilde{t} is related to our t via $\tilde{t} = 2t\hbar$. A detailed analysis reveals furthermore that the \tilde{p} in (3.28) corresponds our $\frac{p}{2}$.

We will start with a numerical analysis of (3.25). Therefore, we plot $\mathcal{A}(z)$, which we define as the absolute value of $W(z)$ divided by the norm to the third, because our graph has three links.

$$\mathcal{A}(z) = \frac{|W(z)|}{\|\psi_g^{\tilde{t}}\|^3}. \quad (3.29)$$

We set $\hbar = \frac{1}{2}$ and truncate the sum (3.25) at $j_{max} = 150$ where one has to make sure that $j_0 < j_{max}$, (3.27) holds. If we set the heatkernel time $t = 1$ we get FIG.(2) and with a

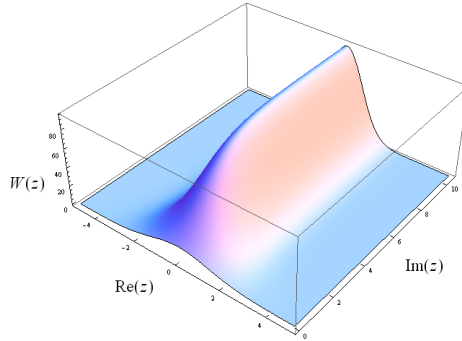


FIG. 2: Normalized amplitude $\mathcal{A}(z)$ for the Cube with $j_{max} = 150$ and $t = 1$

heatkernel time $t = 0.1$ we see that the peak becomes sharper FIG.(3).

Now, recall that $\text{Re}(z)$ corresponds to the extrinsic curvature of our model and thus we find $\text{Re}(z) \propto \dot{a} = 0$ for all volumes $\text{Im}(z) \propto a^2$. Hence, we find that our universe is static. As we would expect. We don't have any matter or a cosmological constant, nor anisotropies.

What is remarkable now is the decrease of the amplitude towards small $\text{Im}(z)$. To see this more clearly insert (3.27) into (3.26) and calculate $\mathcal{A}(z)$ using (3.28). The result is

$$\mathcal{A}(c, p) = \frac{1}{4} \sinh^3 \left(\frac{p}{2} \right) e^{-\frac{3p}{2}} e^{-\frac{3c^2}{8t\hbar}}. \quad (3.30)$$

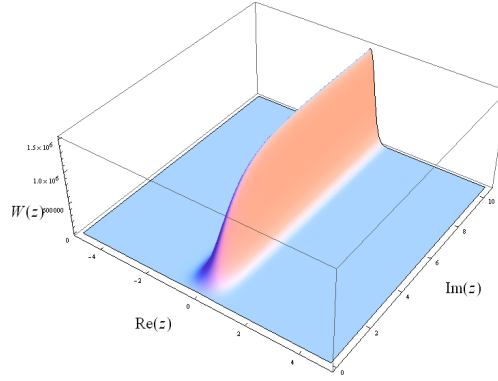


FIG. 3: Normalized amplitude $\mathcal{A}(z)$ for the Cube with $j_{max} = 150$ and $t = 0.1$

Plotting $\mathcal{A}(0, p)$ we get the shape in the p -direction which shows us the drop off for small scale factors FIG.(4).

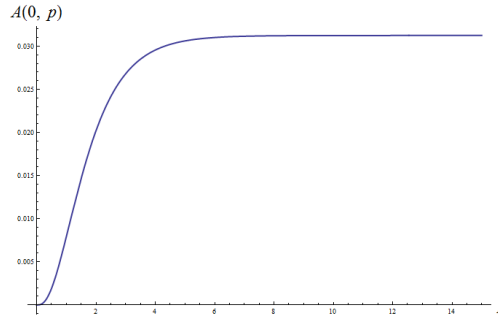


FIG. 4: The transition amplitude as a function of scale factor, for a typical fixed c , here chosen to be zero. We find the amplitude is not supported on $p = 0$, indicating that there can be no transition to singularity.

What does this tell us about the quantum dynamics of our model? Recall the definition of the transition amplitude between two quantum states of geometry Ψ_i and Ψ_f , (3.1). One finds that the main contributions come from those configurations corresponding to classical geometries, namely $\dot{a} = 0$ and large scale factors a . The remarkable result is now, that the transition amplitude decreases for small scale factors and has zero support on $a = 0$. This is a statement about the occurrence of singularities in our model in that it tells us that a transition to a singularity is ruled out dynamically.

The transition amplitude now gives us the possibilities for quantum fluctuations from one scale factor to another one. It doesn't give us the dynamical evolution of our universe. The classical notion of dynamics, i.e. \dot{a} , is encoded in the phase space coordinates. In the same sense as a transition amplitude in QFT does not give us a temporal information of the time evolution of a certain process.

Certainly this result has to be strengthened by future investigations, where it remains to show that one can circumvent the large spin approximation. In fact, one can calculate the traces in (3.9) in our model explicitly, thanks to the fact that our graph has just one node and thus $\langle j, k | \tilde{G} | j, m \rangle = \langle j, k | Y^\dagger \mathcal{D}^{(\gamma j, j)}(G_{s(l)} G_{t(l)}^{-1}) Y | j, m \rangle = \langle (\gamma j, j), j, k | \mathcal{D}^{(\gamma j, j)}(\mathbb{I}) | (\gamma j, j), j, m \rangle = \delta_{km}$ holds. This way one can in principle avoid

the large spin approximation and indeed finds that the amplitude is still peaked on $c = \text{Re}(z) = 0$. However, the shape along the $p = \text{Im}(z)$ direction changes, a problem which probably has to be solved by the use of a different normalization.

IV. DISCUSSION

We showed in this paper that within the spinfoam cosmology approach the Daisy graph is sufficient to reproduce the vacuum Friedmann equation for a flat 3-space in the isotropic setting and thus may also be useful for the investigation of anisotropic models. The Daisy graph is perfectly suited to relax the restriction to isotropic models just by using three different holomorphic labels z_i at each link. This will be our setting in a following paper.

Furthermore, we showed how one can reproduce the missing curvature term in the curved model, described by the Dipole graph, without using higher terms in the spin expansion. The right dependence of the real and imaginary part of the holomorphic labels z will also be important for the description of the anisotropic model. It has been suggested that the curvature term arises as a ‘higher order’ effect in the prior models. However, this derivation applies even in the flat case, which would contradict the agreement with classical dynamics at large scale factor.

The main result of this work, however, is the statement about the avoidance of singularities in our model. The dynamics of the Daisy graph show zero support for a transition amplitude from a finite scale factor to zero, therefore the singularity itself is not accessed by dynamics. Since the model under consideration does not include matter terms, there can be no direct comparison made with the bouncing models of LQC. It remains to be seen at this stage whether this result is an artefact of approximations made, or is a deeper feature of the full covariant dynamics. A singularity resolution theorem or results analogous to those of [6] would be a strong achievement for the theory. In future investigations it has to be clarified, if this result survives if we loosen certain approximations we used in its derivation, and in the following paper we will investigate this in the anisotropic case.

A serious open problem that remains to be investigated within the spinfoam cosmology approach is how to treat higher orders in the vertex expansion and of course the issue of gauge invariance for graphs with more than one node. A key motivation behind the use of the daisy graph is that gauge invariance becomes trivial, a feature due to the symmetries of the spacetime under consideration.

Acknowledgments

The authors would like to thank Carlo Rovelli and Francesca Vidotto for useful comments and discussion. DS gratefully acknowledges support from a Templeton Foundation grant.

Appendix A: Details of the calculations

In this section we present the calculation of the $SL(2, \mathbb{C})$ elements $H_l(z)$, (3.3). As explained in section 2.1 the normal vectors n_l and \tilde{n}_l are obtained via a $SO(3)$ transformation of \hat{e}_z and the $SU(2)$ elements u_l and \tilde{u}_l are related to these $SO(3)$ transformations. We start

with $\hat{e}_z \mapsto \hat{e}_x$ and $\hat{e}_z \mapsto -\hat{e}_x$.

$$\begin{aligned} \begin{pmatrix} 1 \\ 0 \\ 0 \end{pmatrix} &= R_y^{(x)} \hat{e}_z = \begin{pmatrix} \cos(\phi) & 0 & \sin(\phi) \\ 0 & 1 & 0 \\ -\sin(\phi) & 0 & \cos(\phi) \end{pmatrix} \cdot \begin{pmatrix} 0 \\ 0 \\ 1 \end{pmatrix} \\ \phi = \frac{\pi}{2} &\Rightarrow \quad = \begin{pmatrix} 0 & 0 & 1 \\ 0 & 1 & 0 \\ -1 & 0 & 0 \end{pmatrix} \cdot \begin{pmatrix} 0 \\ 0 \\ 1 \end{pmatrix} \end{aligned} \quad (\text{A1})$$

$$\begin{aligned} \begin{pmatrix} -1 \\ 0 \\ 0 \end{pmatrix} &= R_y^{(-x)} \hat{e}_z = \begin{pmatrix} \cos(\phi) & 0 & \sin(\phi) \\ 0 & 1 & 0 \\ -\sin(\phi) & 0 & \cos(\phi) \end{pmatrix} \cdot \begin{pmatrix} 0 \\ 0 \\ 1 \end{pmatrix} \\ \phi = -\frac{\pi}{2} &\Rightarrow \quad = \begin{pmatrix} 0 & 0 & -1 \\ 0 & 1 & 0 \\ 1 & 0 & 0 \end{pmatrix} \cdot \begin{pmatrix} 0 \\ 0 \\ 1 \end{pmatrix} \end{aligned} \quad (\text{A2})$$

We calculate the two corresponding $SU(2)$ elements for the $SO(3)$ rotation matrix R with the formula [35, 36]

$$u = \mp \frac{(\mathbb{I}_2 + \sigma^r \sigma^s R_{rs})}{(2\sqrt{1 + \text{Tr } R})} \in SU(2). \quad (\text{A3})$$

We get for $R_y^{(x)}$ and $R_y^{(-x)}$

$$R_y^{(x)} \rightsquigarrow u^{(x)} = \mp \frac{1}{\sqrt{2}} \begin{pmatrix} 1 & -1 \\ 1 & 1 \end{pmatrix}, \quad (\text{A4})$$

$$R_y^{(-x)} \rightsquigarrow u^{(-x)} = \mp \frac{1}{\sqrt{2}} \begin{pmatrix} 1 & 1 \\ -1 & 1 \end{pmatrix}. \quad (\text{A5})$$

Analogously one calculates $\hat{e}_z \mapsto \hat{e}_y$ and $\hat{e}_z \mapsto -\hat{e}_y$ with the resulting $SU(2)$ elements

$$R_x^{(y)} \rightsquigarrow u^{(y)} = \mp \frac{1}{\sqrt{2}} \begin{pmatrix} 1 & i \\ i & 1 \end{pmatrix} \quad (\text{A6})$$

$$R_x^{(-y)} \rightsquigarrow u^{(-y)} = \mp \frac{1}{\sqrt{2}} \begin{pmatrix} 1 & -i \\ -i & 1 \end{pmatrix}. \quad (\text{A7})$$

Finally, we have to calculate $\hat{e}_z \mapsto \hat{e}_z$ and $\hat{e}_z \mapsto -\hat{e}_z$ but it is clear that $R_y^{(z)}$ is given by

$$R_y^{(z)} = \mathbb{I}_3 \quad (\text{A8})$$

and thus the corresponding $SU(2)$ elements is

$$u^{(z)} = \mp \mathbb{I}_2. \quad (\text{A9})$$

Now we have to connect each two $SU(2)$ elements with one link. We connect those vectors who are co-linear. Furthermore, we need

$$e^{-iz\frac{\sigma^3}{2}} = \begin{pmatrix} e^{-i\frac{z}{2}} & 0 \\ 0 & e^{i\frac{z}{2}} \end{pmatrix}. \quad (\text{A10})$$

The inverse matrices are given by

$$(u^{(-x)})^{-1} = \mp \frac{1}{\sqrt{2}} \begin{pmatrix} 1 & -1 \\ 1 & 1 \end{pmatrix} \quad (\text{A11})$$

$$(u^{(-y)})^{-1} = \mp \frac{1}{\sqrt{2}} \begin{pmatrix} 1 & i \\ i & 1 \end{pmatrix}, \quad (\text{A12})$$

$$(u^{(-z)})^{-1} = \mp \mathbb{I}_2, \quad (\text{A13})$$

where we have chosen (A13) corresponding to the inverse elements of $u^{(x)}$ and $u^{(y)}$ resp. The reason is that formula (A3) is not valid for a rotation of π about the x - or y -axis.

We get for the $SL(2, \mathbb{C})$ elements

$$\begin{aligned} H_1(z) &= u_1 e^{-iz\frac{\sigma^3}{2}} \tilde{u}_1^{-1} = u^{(x)} e^{-iz\frac{\sigma^3}{2}} (u^{(-x)})^{-1} \\ &= \frac{1}{2} \begin{pmatrix} 1 & -1 \\ 1 & 1 \end{pmatrix} \cdot \begin{pmatrix} e^{-i\frac{z}{2}} & 0 \\ 0 & e^{i\frac{z}{2}} \end{pmatrix} \cdot \begin{pmatrix} 1 & -1 \\ 1 & 1 \end{pmatrix} \\ &= \frac{1}{2} \begin{pmatrix} e^{-i\frac{z}{2}} - e^{i\frac{z}{2}} & -e^{-i\frac{z}{2}} - e^{i\frac{z}{2}} \\ e^{-i\frac{z}{2}} + e^{i\frac{z}{2}} & -e^{-i\frac{z}{2}} + e^{i\frac{z}{2}} \end{pmatrix} \\ &= \begin{pmatrix} -i \sin\left(\frac{z}{2}\right) & -\cos\left(\frac{z}{2}\right) \\ \cos\left(\frac{z}{2}\right) & i \sin\left(\frac{z}{2}\right) \end{pmatrix} \\ &= -i \left(\sin\left(\frac{z}{2}\right) \sigma^3 + \cos\left(\frac{z}{2}\right) \sigma^2 \right) \end{aligned} \quad (\text{A14})$$

and for $l = 2$ and $l = 3$ we get analogously

$$\begin{aligned} H_2(z) &= u_2 e^{-iz\frac{\sigma^3}{2}} \tilde{u}_2^{-1} = u^{(y)} e^{-iz\frac{\sigma^3}{2}} (u^{(-y)})^{-1} \\ &= i \left(\cos\left(\frac{z}{2}\right) \sigma^1 - \sin\left(\frac{z}{2}\right) \sigma^3 \right), \end{aligned} \quad (\text{A15})$$

$$\begin{aligned} H_3(z) &= u_3 e^{-iz\frac{\sigma^3}{2}} \tilde{u}_3^{-1} = u^{(z)} e^{-iz\frac{\sigma^3}{2}} (u^{(-z)})^{-1} \\ &= \begin{pmatrix} e^{-i\frac{z}{2}} & 0 \\ 0 & e^{i\frac{z}{2}} \end{pmatrix}. \end{aligned} \quad (\text{A16})$$

- [2] A. Ashtekar, “Gravity and the quantum,” *New Journal of Physics*, vol. 7, no. 1, 2005. <http://stacks.iop.org/1367-2630/7/i=1/a=198>.
- [3] C. Rovelli, “Zakopane lectures on loop gravity,” *arXiv:1102.3660v5 [gr-qc]*, Aug 2011. <http://arxiv.org/abs/1102.3660>.
- [4] A. Ashtekar, T. Pawłowski, and P. Singh, “Quantum nature of the big bang: Improved dynamics,” *Phys. Rev. D*, vol. 74, Oct 2006. <http://link.aps.org/doi/10.1103/PhysRevD.74.084003>.
- [5] M. Bojowald, “Homogeneous loop quantum cosmology,” *Classical and Quantum Gravity*, vol. 20, no. 13, 2003. <http://stacks.iop.org/0264-9381/20/i=13/a=310>.
- [6] P. Singh, “Are loop quantum cosmos never singular?,” *Classical and Quantum Gravity*, vol. 26, no. 12, 2009. <http://stacks.iop.org/0264-9381/26/i=12/a=125005>.
- [7] A. Ashtekar and D. Sloan, “Probability of inflation in loop quantum cosmology,” *General Relativity and Gravitation*, vol. 43, no. 12, 2011. <http://dx.doi.org/10.1007/s10714-011-1246-y>.
- [8] I. Agullo, A. Ashtekar, and W. Nelson, “The pre-inflationary dynamics of loop quantum cosmology: confronting quantum gravity with observations,” *Classical and Quantum Gravity*, vol. 30, no. 8, 2013. <http://stacks.iop.org/0264-9381/30/i=8/a=085014>.
- [9] J. Engle, R. Pereira, and C. Rovelli, “Loop-quantum-gravity vertex amplitude,” *Phys. Rev. Lett.*, vol. 99, Oct 2007. <http://link.aps.org/doi/10.1103/PhysRevLett.99.161301>.
- [10] J. Engle, E. Livine, R. Pereira, and C. Rovelli, “LQG vertex with finite Immirzi parameter,” *Nuclear Physics B*, vol. 799, 2008. <http://www.sciencedirect.com/science/article/pii/S0550321308001405>.
- [11] R. Pereira, “Lorentzian loop quantum gravity vertex amplitude,” *Classical and Quantum Gravity*, vol. 25, no. 8, 2008. <http://stacks.iop.org/0264-9381/25/i=8/a=085013>.
- [12] W. Kaminski, M. Kisielowski, and J. Lewandowski, “Spin-foams for all loop quantum gravity,” *Classical and Quantum Gravity*, vol. 27, no. 9, 2010. <http://stacks.iop.org/0264-9381/27/i=9/a=095006>.
- [13] E. Bianchi, T. Krajewski, C. Rovelli, and F. Vidotto, “Cosmological constant in spinfoam cosmology,” *Phys. Rev. D*, vol. 83, May 2011. <http://link.aps.org/doi/10.1103/PhysRevD.83.104015>.
- [14] A. Baratin, C. Flori, and T. Thiemann, “The holst spin foam model via cubulations,” *New Journal of Physics*, vol. 14, Oct 2012. <http://stacks.iop.org/1367-2630/14/i=10/a=103054>.
- [15] E. Alesci and F. Cianfrani, “Quantum - Reduced Loop Gravity: Cosmology,” *arXiv:1301.2245 [gr-qc]*, Jan 2013. <http://arxiv.org/abs/1301.2245>.
- [16] A. Ashtekar and E. Wilson-Ewing, “Loop quantum cosmology of Bianchi type I models,” *Phys. Rev. D*, vol. 79, Apr 2009. <http://link.aps.org/doi/10.1103/PhysRevD.79.083535>.
- [17] A. Ashtekar and E. Wilson-Ewing, “Loop quantum cosmology of Bianchi type II models,” *Phys. Rev. D*, vol. 80, Dec 2009. <http://link.aps.org/doi/10.1103/PhysRevD.80.123532>.
- [18] E. Wilson-Ewing, “Loop quantum cosmology of Bianchi type IX models,” *Phys. Rev. D*, vol. 82, Aug 2010. <http://link.aps.org/doi/10.1103/PhysRevD.82.043508>.
- [19] A. Corichi and E. Montoya, “Effective dynamics in Bianchi type II loop quantum cosmology,” *Phys. Rev. D*, vol. 85, May 2012. <http://link.aps.org/doi/10.1103/PhysRevD.85.104052>.
- [20] A. Corichi and E. Montoya, “Qualitative effective dynamics in Bianchi II loop quantum cosmology,” *AIP Conference Proceedings*, vol. 1473, no. 1, 2012. <http://link.aip.org/link/APC/1473/113/1>.

- [21] A. Corichi, A. Karami, and E. Montoya, “Loop Quantum Cosmology: Anisotropy and singularity resolution,” *arXiv:1210.7248v2 [gr-qc]*, Dec 2012. <http://arxiv.org/abs/1210.7248>.
- [22] C. Rovelli, *Quantum gravity*. Cambridge monographs on mathematical physics, Cambridge Univ. Press, 2010.
- [23] E. Bianchi, E. Magliaro, and C. Perini, “Spinfoams in the holomorphic representation,” *Phys. Rev. D*, vol. 82, Dec 2010. <http://link.aps.org/doi/10.1103/PhysRevD.82.124031>.
- [24] E. R. Livine and S. Speziale, “New spinfoam vertex for quantum gravity,” *Phys. Rev. D*, vol. 76, Oct 2007. <http://link.aps.org/doi/10.1103/PhysRevD.76.084028>.
- [25] E. Bianchi, E. Magliaro, and C. Perini, “Coherent spin-networks,” *Phys. Rev. D*, vol. 82, Jul 2010. <http://link.aps.org/doi/10.1103/PhysRevD.82.024012>.
- [26] M. Bojowald, “Loop quantum cosmology: I. kinematics,” *Classical and Quantum Gravity*, vol. 17, no. 6, 2000. <http://stacks.iop.org/0264-9381/17/i=6/a=312>.
- [27] M. Bojowald, “Isotropic loop quantum cosmology,” *Classical and Quantum Gravity*, vol. 19, no. 10, 2002. <http://stacks.iop.org/0264-9381/19/i=10/a=313>.
- [28] M. Bojowald, G. Date, and K. Vandersloot, “Homogeneous loop quantum cosmology: the role of the spin connection,” *Classical and Quantum Gravity*, vol. 21, no. 4, 2004. <http://stacks.iop.org/0264-9381/21/i=4/a=034>.
- [29] T. Thiemann and O. Winkler, “Gauge field theory coherent states (GCS): II. Peakedness properties,” *Classical and Quantum Gravity*, vol. 18, no. 14, 2001. <http://stacks.iop.org/0264-9381/18/i=14/a=301>.
- [30] T. Thiemann, *Modern Canonical Quantum General Relativity*. Cambridge monographs on mathematical physics, Cambridge University Press, 1st ed., 2008.
- [31] F. Hellmann, “Expansions in spin foam cosmology,” *Phys. Rev. D*, vol. 84, Nov 2011. <http://link.aps.org/doi/10.1103/PhysRevD.84.103516>.
- [32] M. Kisielowski, J. Lewandowski, and J. Puchta, “One vertex spin-foams with the dipole cosmology boundary,” *arXiv:1203.1530v1 [gr-qc]*, Mar 2012. <http://arxiv.org/abs/1203.1530>.
- [33] J. Engle and R. Pereira, “Regularization and finiteness of the lorentzian loop quantum gravity vertices,” *Phys. Rev. D*, vol. 79, Apr 2009. <http://link.aps.org/doi/10.1103/PhysRevD.79.084034>.
- [34] D. M. Brink and G. R. Satchler, *Angular Momentum*. Oxford University Press, USA, 3 ed., Mar 1994.
- [35] M. Carmeli, *Group Theory and General Relativity - Representations of the Lorentz Group and Their Applications to the Gravitational Field*. McGraw-Hill Inc.,US, Aug 1977.
- [36] R. U. Sexl and H. K. Urbantke, *Relativity, Groups, Particles: Special Relativity - Relativistic Symmetry in Field and Particle Physics*. Springer, 1 ed., Nov 2000.